# Importance of the Breit Interaction for Electron–Positron Pair Production in Bound–Bound Muon Transitions

Oleg Yu. Andreev[1,2,3], Deyang Yu (于得洋)[1,4*], Konstantin N. Lyashchenko[1,3,2], and Daria M. Vasileva[3,2]

[1]*Institute of Modern Physics, Chinese Academy of Sciences, Lanzhou 730000, China*
[2]*St. Petersburg State University, 7/9 Universitetskaya nab., St. Petersburg 199034, Russia*
[3]*Petersburg Nuclear Physics Institute named by B.P. Konstantinov of National Research Centre "Kurchatov Institute", Gatchina 188300, Russia*
[4]*University of Chinese Academy of Sciences, Beijing 100049, China*

(Received 10 April 2025; accepted manuscript online 4 July 2025)

We explored a distinct mechanism for matter creation via electron–positron pair production during bound–bound transitions in the deexcitation of muonic atoms. For ions with nuclear charges $Z \geqslant 24$, transitions from low-lying excited states to the 1s-muon state can lead to the production of electron–positron pairs. We show that the Breit interaction determines the transition probabilities for states with nonzero orbital momentum. We show that the pair production arises mainly from the decay of the 2p states. Thus, the Breit interaction governs electron–positron pair production in bound-bound muon transitions. This process offers a unique opportunity to explore quantum electrodynamics in strong fields, as well as a class of nonradiative transitions involving electron–positron pair production.

DOI: 10.1088/0256-307X/42/9/090301 CSTR: 32039.14.0256-307X.42.9.090301

Muonic ions and atoms represent a significant area of research in modern physics.[1–4] While muonic ions share many similarities with one-electron ions, including a theoretical description that closely parallels electronic systems,[5,6] they exhibit important qualitative differences. These differences arise from the finite lifetime of the muon, nuclear effects such as finite nuclear size and recoil, and the distinct energy scales of muonic ions. The muon, being about 207 times more massive than the electron,[7] has an orbital radius 100 to 200 times smaller than that of an electron.[8,9] This results in a much stronger interaction with the nucleus, leading to greater energy release during the decay of excited states compared to conventional electronic systems. In particular, the transition energies of muons can be large enough to produce electron–positron pairs, introducing a unique decay channel for matter creation that is not present in bound-bound transitions of few-electron ions.

The decay channels for bound muons were analyzed by Wheeler.[8] Some of these decay processes are shared with one-electron ions, while others are specific to muonic ions. We emphasize that experimentally, only ions containing a single bound muon are observed. In medium and heavy ions, the primary decay channels for excited states in one-muon ions are radiative decays.[8,9] In light muonic ions, where electrons are present in addition to the muon, Auger decay can play a significant role. In this paper, we investigate an additional decay channel for muonic ions, arising from their specific energy range: pair-production transitions in which the excess energy is used to produce an electron–positron pair. This type of decay for the 2s muon state was previously considered in Ref. [8]. Using QED framework, we examine the decays of muonic states with principal quantum numbers $n = 2$ and 3, demonstrating that the dominant transitions for electron–positron pair production are the $2p \to 1s$ transitions. The significance of these transitions is largely due to the substantial contribution of the Breit interaction for the 2p states.

Testing QED in strong fields is a pressing and widely discussed issue.[10–13] Most of these studies focus on photon emission processes, specifically measurements of photon frequencies which are used to determine energy levels and $g$-factors. Investigating transitions where excess energy is carried away by electron–positron pairs is both highly important and promising. Such studies provide a unique opportunity to explore a largely unexplored branch of QED, potentially offering new insights into fundamental processes in strong-field regimes.

Electron–positron pair production in these muonic transitions has not yet been studied experimentally. Previous research into pair production in atomic physics has primarily focused on its occurrence in relativistic collisions of heavy nuclei with atoms (dynamic pair production).[14–20]

Recent advances have demonstrated the unique potential of muonic systems for testing QED, particularly through Rydberg states of muonic atoms.[21,22]

Significant efforts have been devoted to observing the mechanism of spontaneous electron–positron pair produc-

*Corresponding author. Email: d.yu@impcas.ac.cn
© 2025 Chinese Physical Society and IOP Publishing Ltd. All rights, including for text and data mining, AI training, and similar technologies, are reserved.

tion, which may occur during slow collisions of heavy nuclei.[23–25] This mechanism is based on the theoretical prediction that for nuclear charges $Z \geqslant 174$ 1s-electron state energy drops below $-m_e c^2$ (where $m_e$ is the electron mass), making spontaneous pair production energetically favorable. However, this phenomenon has not yet been experimentally confirmed.

The nonradiative electron–positron pair production transitions, can be schematically described as

$$\mu_i \to \mu_f + e^-(\varepsilon) + e^+(\varepsilon') \,. \tag{1}$$

The initial (i) and final (f = 1 s) states of the muon are denoted as $\mu_i$ and $\mu_f$, respectively. The produced electron and positron are described by their energy ($\varepsilon$, $\varepsilon'$), momentum ($\boldsymbol{p}$, $\boldsymbol{p}'$) and polarization ($\mu$ and $\mu'$).[26] The energy release during transitions between the different states can be estimated by the (nonrelativistic) Bohr formula for the energy levels of one-electron ions. This shows that if the atomic number $Z$ is larger or equal to 22 (the more precise calculation predicts $Z \geqslant 24$), then the energy release becomes greater than $2m_e c^2$, which is enough to produce an electron–positron pair. The energy conservation law reads

$$\Delta\varepsilon^{(\mu)}_{i\to 1s} = \varepsilon^{(\mu)}_i - \varepsilon^{(\mu)}_{1s} = \varepsilon + \varepsilon' > 2m_e c^2 \,. \tag{2}$$

Our study focuses exclusively on electron–positron pair production where the electron belongs to the continuum part of the Dirac spectrum. First, in an experimental setup, a muon beam collides with atoms, and the muon can be treated as bound to the nucleus without significantly affecting the atomic electrons, since its orbital radius is much smaller. Thus, many low-lying electron states are occupied, and capture into these states is forbidden by the Pauli principle. Second, the contribution of unoccupied bound electron states to the total muon transition probability is relatively small.

We consider the muon transition involving the electron–positron pair production, given by Eq. (1), within the framework of QED theory. The Furry picture is used,[27] in which the interaction between particles and the electric field of the atomic nucleus is fully taken into account. In the lowest order of the QED perturbation theory, the amplitude of this process can be written as (in the Feynman gauge)[26,28]

$$A_{i\to f} = e^2 \int \mathrm{d}\boldsymbol{r}_1 \mathrm{d}\boldsymbol{r}_2 \psi^{(-)\dagger}_{\varepsilon,\boldsymbol{p}\mu}(\boldsymbol{r}_1)\phi^\dagger_f(\boldsymbol{r}_2)(1-\boldsymbol{\alpha}^{(1)}\boldsymbol{\alpha}^{(2)}) \times \frac{\mathrm{e}^{\mathrm{i}\frac{\omega r_{12}}{c}}}{r_{12}} \psi^{(-)}_{-\varepsilon',-\boldsymbol{p}'\mu'}(\boldsymbol{r}_1)\phi_i(\boldsymbol{r}_2) \,, \tag{3}$$

where $\omega = (\varepsilon + \varepsilon')/\hbar$, $r_{12} = |\boldsymbol{r}_1 - \boldsymbol{r}_2|$, $\boldsymbol{\alpha}^{(i)}$ are the Dirac $\alpha$-matrices acting on the wave functions with the argument $\boldsymbol{r}_i$. The wave functions $\phi_{i,f}(\boldsymbol{r}_2)$ represent the muon in its initial and final states. The wave function $\psi^{(-)}_{\varepsilon,\boldsymbol{p}\mu}(\boldsymbol{r}_1)$ describes the emitted electron, and $\psi^{(-)}_{-\varepsilon',-\boldsymbol{p}'\mu'}(\boldsymbol{r}_1)$ corresponds to the emitted positron.[26] The Coulomb interaction is obtained by setting $\omega = 0$ and neglecting the $\boldsymbol{\alpha}^{(1)}\boldsymbol{\alpha}^{(2)}$ term.

The transition probably can be written as[26]

$$\mathrm{d}w^{(e^+e^-)}_{i\to 1s} = \frac{2\pi}{\hbar}\delta(\varepsilon^{(\mu)}_i - \varepsilon^{(\mu)}_f - \varepsilon - \varepsilon') \times |A_{i\to f}|^2 \frac{\mathrm{d}\boldsymbol{p}\,\mathrm{d}\boldsymbol{p}'}{(2\pi\hbar)^6} \,. \tag{4}$$

By integrating over the electron and positron momenta, averaging over the projections of the total angular momentum of the initial muon state, and summing over the final states (including different polarizations of the produced electron and positron, as well as the projections of the muon total angular momentum), we obtain the total transition probability $w^{(e^+e^-)}$.

We accounted for the nuclear size corrections using the Fermi distribution for the nuclear charge density. In the framework of the lowest-order QED perturbation theory, three radiative corrections must be taken into account: the muon self-energy correction, the electron-loop vacuum polarization correction, and the muon-loop vacuum polarization correction. Both the muon self-energy correction and the muon-loop vacuum polarization include the creation and annihilation of virtual muons. Because of the large mass of the muon relative to the electron, these contributions are significantly suppressed compared to the electron-loop vacuum polarization. Therefore, we include in our calculations only the dominant electron-loop contribution, treating it in the Uehling approximation.[29]

The transition probabilities for the decay of the 2s-muon states with electron–positron pair production were considered by Wheeler[8] within the nonrelativistic limit and for point-like nucleus are presented in the following (in $\mathrm{s}^{-1}$), where our results are given in parentheses. The digits in square brackets indicate powers of 10,

$$\begin{aligned} w^{(e^+e^-,Z=25)}_{2s\to 1s} &\approx 2[8]\ (5.54[8]), \\ w^{(e^+e^-,Z=30)}_{2s\to 1s} &\approx 5[10]\ (2.46[10]), \\ w^{(e^+e^-,Z=35)}_{2s\to 1s} &\approx 8[11]\ (1.25[11]), \\ w^{(e^+e^-,Z=40)}_{2s\to 1s} &\approx 5[12]\ (3.87[11]). \end{aligned}$$

We can see, that the $Z$-dependence of the transition probabilities calculated within the QED differs significantly from the prediction of the nonrelativistic limit.[8]

In Fig. 1, we present the radiative transition probabilities for the $2p_{1/2}$, $2p_{3/2}$, and $2s_{1/2}$ states, along with the nonradiative electron–positron pair production transition probabilities, as functions of $Z$. The figure also includes branching ratios for transitions involving electron–positron pair production. We can see that for $Z \geqslant 36$, the branching ratio for the 2p states exceeds that for the 2s states. This is attributed to two main factors: the importance of nuclear size corrections for bound muons and the very large contribution of the Breit interaction for 2p-muon states.

Numerically calculated transition probabilities (in $\mathrm{s}^{-1}$) and transition energies (in $m_e c^2$) for one-muon ions are provided in Table 1. We analyze the decay of low-lying muon states with $n = 2$ and $n = 3$ for $Z = 24$, 36, 54 and 92. The initial one-muon states (i) are indicated in the first row of the table.

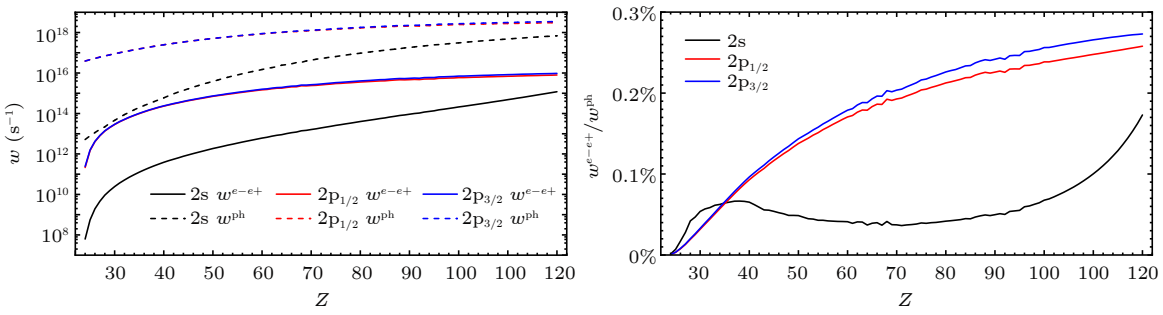


**Fig. 1.** Transition probabilities for excited muon states ($i$): $2p_{1/2}$ (red curves), $2p_{3/2}$ (blue curves), and 2s (black curves). On the upper panel, the radiative transition probabilities $W_i$ in s$^{-1}$ (dashed curves) and the nonradiative electron–positron pair production transition probabilities $w_{i\to 1s}^{(e^+e^-)}$ in s$^{-1}$ (solid curves) as functions of the nucleus atomic number $Z$. The bottom panel shows the ratio between the nonradiative and radiative transition probabilities $w_{i\to 1s}^{(e^+e^-)}/w_i^{(\gamma)}$.

The total energies of the 1s-muon states ($\varepsilon_{1s}^{(\mu)}$), including the rest mass of muon, are given explicitly for each $Z$ values. The row marked $\Delta\varepsilon_{i\to 1s}^{(\mu)}$ shows the energy difference $\Delta\varepsilon_{i\to 1s}^{(\mu)} = \varepsilon_i^{(\mu)} - \varepsilon_{1s}^{(\mu)}$, where i is the corresponding initial state. This difference represents the energy available for electron–positron pair production. Deviations from the Bohr formula are mainly due to nuclear effects. Incorporating nuclear size corrections significantly alters the order and energy differences of one-muon energy levels, resulting in notably different radiative transition probabilities compared to those for one-electron ions.[9]

The row $w_i^{(\gamma)}$ represents the total radiative transition probability for transitions from initial (excited) state i to all lower states.

The row labeled $w_{i\to 1s}^{(e^+e^-)}$ presents the full QED calculation of the transition probabilities for the nonradiative electron–positron pair production transitions from the initial states i to the 1s-muon state Eq. (1) The rows labeled $w_{i\to 1s}^{(e^+e^-)C}$ show these transition probabilities when only the Coulomb interaction is considered. The difference between the exact interelectron interaction and the Coulomb interaction reflects the contribution of the Breit interaction. We observe that the Breit interaction has a minimal effect on the decay of 2s and 3s muon states. However, it significantly impacts the decay of muon states with orbital momentum $l \geq 1$. Specifically, for 2p states, the Breit interaction increases the transition probabilities $w_{i\to 1s}^{(e^+e^-)}$ by a factor of 2.8 for $Z = 24$ and by a factor of 7.6 for $Z = 92$. These increases in transition probabilities lead to substantial changes in the patterns of electron–positron pair production in muon ions.

In addition to direct electron–positron pair production, described by Eq. (1), transitions that involve electron–positron pair production alongside photon emission are also significant for many states. In the dominant cascade channel, these transitions can be represented as follows:

$$\mu_i \to \mu_n + \gamma \to \mu_{1s} + e^-(\varepsilon) + e^+(\varepsilon') + \gamma(\omega)\,, \quad (5)$$

where $n$ represents an intermediate state between the initial state i and the final 1s state. The transition probabilities for these processes are denoted as $w_{i\to n\to 1s}^{(\gamma,e^+e^-)}$ and are provided in the corresponding rows of Table 1 (for $n = 2p_{1/2}$, $2p_{3/2}$, and 2s). Restricting our analysis to the cascade channel, we calculate these transition probabilities as follows:

$$w_{i\to n\to 1s}^{(\gamma,e^+e^-)} = w_{i\to n}^{(\gamma)} \frac{w_{n\to 1s}^{(e^+e^-)}}{w_n^{(\gamma)}}\,, \quad (6)$$

where $w_n^{(\gamma)}$ is the total radiative transition probability for the transition from state $n$. These values are provided in Table 1. Since the Breit interaction significantly increases the transition probabilities $w_{n\to 1s}^{(e^+e^-)}$ (for states with the orbital momentum $l \geq 1$), it also substantially enhances the $w_{i\to n\to 1s}^{(\gamma,e^+e^-)}$ transition probabilities.

The increase in transition probabilities results in most electron–positron pairs being produced in the 2p → 1s transitions. Table 1 and Fig. 1 show that for ions with $Z \geq 36$, even if the muon initially occupies the 2s state, the production of an electron–positron pair in the 2p → 1s transitions is more frequent than in the 2s → 1s transition. The cascade channel 2s → 2p → 1s includes two transitions, $2p_{1/2} \to 1s$ and $2p_{3/2} \to 1s$, whose combined probability ($w_{2s\to 2p_{1/2}\to 1s}^{(\gamma,e^+e^-)} + w_{2s\to 2p_{3/2}\to 1s}^{(\gamma,e^+e^-)}$) is higher than that of the direct 2s → 1s transition ($w_{2s\to 1s}^{(e^+e^-)}$).

Assuming that the excited bound muon states are relatively evenly populated in experiments on muon capture by atoms, we can conclude that most electron–positron pairs are produced during the 2p → 1s transitions for all atomic numbers $Z \geq 24$. Specifically, taking into account the cascade transitions described by Eq. (5), which involve photon emission and electron–positron pair production, from the 3s, 3p, and 3d states, we obtain that electron–positron pair production predominantly occurs during the 2p → 1s transitions. The corresponding transition probabilities are shown in Table 1.

Since the total energy of the electron–positron pair produced in a bound-bound muon transition is determined by the energy conservation law, the technique of simultaneously detecting both the electron and positron while analyzing their combined energy can help identify pairs produced in specific bound-bound muon transitions. The time projection chamber technique[30] offers a promising approach for this purpose, particularly when employing gas targets, such as krypton ($_{36}$Kr) and xenon ($_{54}$Xe).

**Table 1.** Transition probabilities (in $\mathrm{s}^{-1}$) for one-muon ions. The digits in square brackets indicate powers of 10. The first row lists the initial (excited) states (i). The total energies of the 1s-muon states $\varepsilon_{1s}^{(\mu)}$, including the rest mass of muon, are given explicitly for each $Z$ value. The row labeled $\Delta\varepsilon_{i\to 1s}^{(\mu)}$ shows the energy differences $\Delta\varepsilon_{i\to 1s}^{(\mu)} = \varepsilon_{i}^{(\mu)} - \varepsilon_{1s}^{(\mu)}$ (in $m_e c^2$), where $\varepsilon_{i}^{(\mu)}$ represent the total energies of the initial (i) muon states. The row $w_{i}^{(\gamma)}$ represents the total radiative transition probability for transitions from state i to all lower states. The row $w_{i\to 1s}^{(e^+e^-)}$ provides the transition probabilities for the nonradiative electron–positron pair production transitions [from the initial (excited) state i to the 1s muon state] as described in Eq. (1), while $w_{i\to 1s}^{(e^+e^-)\mathrm{C}}$ gives these transition probabilities considering only the Coulomb interaction. The row $w_{i\to n\to 1s}^{(\gamma,e^+e^-)}$ present the transition probabilities for radiative cascade transitions $\mathrm{i}\to n\to 1\mathrm{s}$ involving electron–positron pair production as described in Eq. (5), where i refers to the states listed in the first row.

| | $2p_{1/2}$ | $2p_{3/2}$ | $2s_{1/2}$ | $3p_{1/2}$ | $3d_{3/2}$ | $3p_{3/2}$ | $3d_{5/2}$ | $3s_{1/2}$ |
|---|---|---|---|---|---|---|---|---|
| | | | $Z = 24$, | $\varepsilon_{1s}^{(\mu)} = 203.8292$ | | | | |
| $\Delta\varepsilon_{i\to 1s}^{(\mu)}$ | 2.1362 | 2.1421 | 2.1717 | 2.5833 | 2.5852 | 2.5851 | 2.5858 | 2.5939 |
| $w_{i}^{(\gamma)}$ | 3.97[16] | 3.94[16] | 4.95[12] | 1.17[16] | 4.54[15] | 1.17[16] | 4.49[15] | 2.78[14] |
| $w_{i\to 1s}^{(e^+e^-)}$ | 2.14[11] | 2.42[11] | 6.23[7] | 1.19[12] | 6.73[8] | 1.22[12] | 6.77[8] | 5.71[8] |
| $w_{i\to 1s}^{(e^+e^-)\mathrm{C}}$ | 7.65[10] | 8.55[10] | 6.22[7] | 3.35[11] | 2.21[8] | 3.45[11] | 2.23[8] | 5.71[8] |
| $w_{i\to 2p_{1/2}\to 1s}^{(\gamma,e^+e^-)}$ | | 1.67[1] | 1.22[7] | 3.71[1] | 2.04[10] | 2.61[6] | 6.79[3] | 4.70[8] |
| $w_{i\to 2p_{3/2}\to 1s}^{(\gamma,e^+e^-)}$ | | | 1.63[7] | 5.90[6] | 4.57[9] | 2.93[6] | 2.75[10] | 1.17[9] |
| $w_{i\to 2s\to 1s}^{(\gamma,e^+e^-)}$ | | | | 2.10[10] | 2.10[7] | 2.05[10] | 2.11[7] | 2.27[2] |
| | | | $Z = 36$, | $\varepsilon_{1s}^{(\mu)} = 200.7596$ | | | | |
| $\Delta\varepsilon_{i\to 1s}^{(\mu)}$ | 4.1839 | 4.2119 | 4.3563 | 5.2018 | 5.2093 | 5.2099 | 5.2124 | 5.2536 |
| $w_{i}^{(\gamma)}$ | 1.75[17] | 1.74[17] | 2.46[14] | 4.96[16] | 2.34[16] | 5.04[16] | 2.29[16] | 6.91[14] |
| $w_{i\to 1s}^{(e^+e^-)}$ | 1.20[14] | 1.23[14] | 1.62[11] | 4.08[13] | 1.53[11] | 4.28[13] | 1.52[11] | 7.07[10] |
| $w_{i\to 1s}^{(e^+e^-)\mathrm{C}}$ | 2.47[13] | 2.55[13] | 1.61[11] | 7.27[12] | 2.96[10] | 7.74[12] | 3.00[10] | 7.04[10] |
| $w_{i\to 2p_{1/2}\to 1s}^{(\gamma,e^+e^-)}$ | | 2.20[5] | 7.60[10] | 2.78[5] | 1.33[13] | 3.84[9] | 2.32[7] | 1.23[11] |
| $w_{i\to 2p_{3/2}\to 1s}^{(\gamma,e^+e^-)}$ | | | 9.59[10] | 7.79[9] | 2.67[12] | 3.85[9] | 1.60[13] | 3.35[11] |
| $w_{i\to 2s\to 1s}^{(\gamma,e^+e^-)}$ | | | | 5.75[12] | 9.50[9] | 5.57[12] | 9.66[9] | 4.74[5] |
| | | | $Z = 54$, | $\varepsilon_{1s}^{(\mu)} = 195.2742$ | | | | |
| $\Delta\varepsilon_{i\to 1s}^{(\mu)}$ | 7.3448 | 7.4593 | 8.0501 | 9.6624 | 9.6805 | 9.6941 | 9.6964 | 9.8765 |
| $w_{i}^{(\gamma)}$ | 6.47[17] | 6.54[17] | 7.08[15] | 1.69[17] | 1.21[17] | 1.79[17] | 1.15[17] | 1.44[15] |
| $w_{i\to 1s}^{(e^+e^-)}$ | 9.60[14] | 1.01[15] | 3.04[12] | 2.41[14] | 3.75[12] | 2.71[14] | 3.66[12] | 1.15[12] |
| $w_{i\to 1s}^{(e^+e^-)\mathrm{C}}$ | 1.42[14] | 1.52[14] | 3.01[12] | 3.05[13] | 4.72[11] | 3.55[13] | 4.84[11] | 1.13[12] |
| $w_{i\to 2p_{1/2}\to 1s}^{(\gamma,e^+e^-)}$ | | 3.22[7] | 4.64[12] | 3.15[7] | 1.48[14] | 9.54[10] | 1.34[9] | 4.54[9] |
| $w_{i\to 2p_{3/2}\to 1s}^{(\gamma,e^+e^-)}$ | | | 6.13[12] | 1.91[11] | 2.90[13] | 9.42[10] | 1.75[14] | 3.19[11] |
| $w_{i\to 2s\to 1s}^{(\gamma,e^+e^-)}$ | | | | 1.81[13] | 4.06[10] | 1.76[13] | 4.26[10] | 9.72[6] |
| | | | $Z = 92$, | $\varepsilon_{1s}^{(\mu)} = 183.183$ | | | | |
| $\Delta\varepsilon_{i\to 1s}^{(\mu)}$ | 12.160 | 12.607 | 15.314 | 18.579 | 18.392 | 18.692 | 18.521 | 19.561 |
| $w_{i}^{(\gamma)}$ | 2.13[18] | 2.32[18] | 2.09[17] | 4.88[17] | 9.50[17] | 5.71[17] | 8.85[17] | 6.21[16] |
| $w_{i\to 1s}^{(e^+e^-)}$ | 4.72[15] | 5.51[15] | 1.05[14] | 7.28[14] | 1.02[14] | 9.96[14] | 9.84[13] | 4.10[13] |
| $w_{i\to 1s}^{(e^+e^-)\mathrm{C}}$ | 6.04[14] | 7.22[14] | 1.02[14] | 8.43[13] | 9.66[12] | 1.20[14] | 1.04[13] | 3.95[13] |
| $w_{i\to 2p_{1/2}\to 1s}^{(\gamma,e^+e^-)}$ | | 2.78[9] | 1.92[14] | 3.70[9] | 1.71[15] | 3.08[12] | 1.10[11] | 2.56[13] |
| $w_{i\to 2p_{3/2}\to 1s}^{(\gamma,e^+e^-)}$ | | | 2.91[14] | 6.09[12] | 3.24[14] | 3.03[12] | 2.00[15] | 2.71[13] |
| $w_{i\to 2s\to 1s}^{(\gamma,e^+e^-)}$ | | | | 1.15[14] | 2.16[11] | 1.20[14] | 2.72[11] | 6.74[8] |

Data for these gases are provided in Table 1. Another possible experimental approach to studying this effect is to examine collisions of muons with thin foils of elements with $Z \geqslant 24$, or foils of light atoms containing impurities of heavier elements. Determining that both particles come from a single electron–positron pair with a fixed total energy can be achieved using coincidence detection methods.[31]

In summary, we have explored a mechanism for matter creation through the decay of muonic ions, where the excess energy is emitted as an electron–positron pair. Our calculations, based on QED and incorporating nuclear corrections, reveal that the Breit interaction plays a crucial role in decays of states with orbital angular momentum $l \geqslant 1$, increasing the corresponding transition probabilities by a factor of 3 to 7. Moreover, the inclusion of the Breit interaction significantly alters the pattern of electron–positron pair production in muonic ion decays. Numerical analysis shows that the dominant contributions to pair production come from the decay of 2p states.

While it is generally assumed that atomic processes are primarily governed by the Coulomb interaction with the Breit interaction providing only a minor correction, we have identified a class of processes in which the Breit interaction plays a dominant role. This enhances our understanding of fundamental interactions and may have important implications for many-particle physics.

Bound–bound muon transitions involving electron–positron pair production represent a distinct branch of QED that remains largely unexplored and holds the potential for uncovering significant physical phenomena. As the branching ratio of electron–positron pair production reaches the order of $10^{-3}$, experimental studies of this process at modern muon facilities[3,4] can be expected in the near future.

*Acknowledgements.* The authors thank Prof. Jianmin Dong for valuble discussions. D.M.V. expresses gratitude for the hospitality of the Institute of Modern Physics of Chinese Academy of Sciences during her visit. This work was supported by the National Key Research and Development Program of China (Grant No. 2022YFA1602501) and the National Natural Science Foundation of China (Grant No. 12011530060). The work of O.Y.A., K.N.L., D.M.V. in part of the calculation of the radial integrals was supported solely by the Russian Science Foundation (Grant No. 22-12-00043). O.Y.A. and K.N.L. were supported by the Chinese Academy of Sciences (CAS) Presidents International Fellowship Initiative (PIFI) (Grant Nos. 2018VMB0016 and 2022VMC0002), respectively.

# References

[1] Nagamine K 2003 (Cambridge: Cambridge University Press)
[2] Gorringe T and Hertzog D 2015 *Prog. Part. Nucl. Phys.* **84** 73
[3] Bao Y, Chen J, Chen C, Cheng H, Deng C, Fan R, Guo Y, He N, Hu H, Li Q, Li Y, Liang H, Liu L, Lv Y, Pan Z, Tan Z, Vassilopoulos N, Wu Y, Yang T, and Zhang G 2023 *J. Phys.: Conf. Ser.* **2462** 012034
[4] Cai H J, He Y, Liu S, Jia H, Qin Y, Wang Z, Wang F, Zhao L, Pu N, Niu J, Chen L, Sun Z, Zhao H, and Zhan W 2024 *Phys. Rev. Accel. Beams* **27** 023403
[5] Mohr P J, Plunien G, and Soff G 1998 *Phys. Rep.* **293** 227
[6] Oreshkina N S 2022 *Phys. Rev. Res.* **4** L042040
[7] Tiesinga E, Mohr P J, Newell D B, and Taylor B N 2021 *Rev. Mod. Phys.* **93** 025010
[8] Wheeler J A 1949 *Rev. Mod. Phys.* **21** 133
[9] Knyazeva V A, Lyashchenko K N, Zhang M, Yu D, and Andreev O Yu 2022 *Phys. Rev. A* **106** 012809
[10] Morgner J, Tu B, König C M, Sailer T, Heiβe F, Bekker H, Sikora B, Lyu C, Yerokhin V A, Harman Z, López-Urrutia J R C, Keitel C H, Sturm S, and Blaum K 2023 *Nature* **622** 53
[11] Loetzsch R, Beyer H F, Duval L, Spillmann U, Banaś D, Dergham P, Kröger F M, Glorius J, Grisenti R E, Guerra M, Gumberidze A, Heβ R, Hillenbrand P M, Indelicato P, Jagodzinski P, Lamour E, Lorentz B, Litvinov S, Litvinov Yu A, Machado J, Paul N, Paulus G G, Petridis N, Santos J P, and Trassinelli M 2024 *Nature* **625** 673
[12] Morgner J, Tu B, Moretti M, König C M, Heiβe F, Sailer T, Yerokhin V A, Sikora B, Oreshkina N S, Harman Z, Keitel C H, Sturm S, and Blaum K 2025 *Phys. Rev. Lett.* **134** 123201
[13] Pfafflein P, Weber G, Allgeier S, Andelkovic Z, Bernitt S, Bondarev A I, Borovik A, Duval L, Fleischmann A, Forstner O, Friedrich M, Glorius J, Gumberidze A, Hahn C, Herfurth F, Hengstler D, Herdrich M O, Hillenbrand P-M, Kalinin A, Kiffer M, Kröger F M, Kubullek M, Kuntz P, Lestinsky M, Litvinov Y A, Löher B, Menz E B, Over T, Petridis N, Ringleb S, Sidhu R S, Spillmann U, Trotsenko S, Warczak A, Zhu B, Enss C, and Stöhlker T 2025 *Phys. Rev. Lett.* **134** 153001
[14] Belkacem A, Gould H, Feinberg B, Bossingham R, and Meyerhof W E 1993 *Phys. Rev. Lett.* **71** 1514
[15] Belkacem A, Gould H, Feinberg B, Bossingham R, and Meyerhof W E 1994 *Phys. Rev. Lett.* **73** 2432
[16] Belkacem A, Gould H, Feinberg B, Bossingham R, and Meyerhof W E 1997 *Phys. Rev. A* **56** 2806
[17] Belkacem A, Claytor N, Dinneen T, Feinberg B, and Gould H 1998 *Phys. Rev. A* **58** 1253
[18] Bethe H A and Maximon L C 1954 *Phys. Rev.* **93** 768
[19] Decker F 1991 *Phys. Rev. A* **44** 2883
[20] Decker F and Eichler J 1992 *Phys. Rev. A* **45** 3343
[21] Paul N, Bian G, Azuma T, Okada S, and Indelicato P 2021 *Phys. Rev. Lett.* **126** 173001
[22] Okumura T, Azuma T, Bennett D A, Chiu I, Doriese W B, Durkin M S, Fowler J W, Gard J D, Hashimoto T, Hayakawa R, Hilton G C, Ichinohe Y, Indelicato P, Isobe T, Kanda S, Katsuragawa M, Kawamura N, Kino Y, Mine K, Miyake Y, Morgan K M, Ninomiya K, Noda H, O'Neil G C, Okada S, Okutsu K, Paul N, Reintsema C D, Schmidt D R, Shimomura K, Strasser P, Suda H, Swetz D S, Takahashi T, Takeda S, Takeshita S, Tampo M, Tatsuno H, Ueno Y, Ullom J N, Watanabe S, and Yamada S 2023 *Phys. Rev. Lett.* **130** 173001
[23] Maltsev I A, Shabaev V M, Popov R V, Kozhedub Y S, Plunien G, Ma X, Stöhlker T, and Tumakov D A 2019 *Phys. Rev. Lett.* **123** 113401
[24] Shabaev V, Bondarev A, Glazov D, Kozhedub Y, Maltsev I, Malyshev A, Popov R, Tumakov D, and Tupitsyn I 2019 *PoS* **FFK2019** 353
[25] Dulaev N K, Telnov D A, Shabaev V M, Kozhedub Y S, Ma X, Maltsev I A, Popov R V, and Tupitsyn I I 2025 *Phys. Rev. D* **111** 016018
[26] Akhiezer A I and Berestetskii V B 1965 *Quantum Electrodynamics* (New York: Wiley Interscience)
[27] Furry W H 1951 *Phys. Rev.* **81** 115
[28] Andreev O Yu, Labzowsky L N, Plunien G, and Solovyev D A 2008 *Phys. Rep.* **455** 135
[29] Uehling E A 1935 *Phys. Rev.* **48** 55
[30] Doke T 1993 *Nucl. Instrum. Methods Phys. Res. A* **327** 113
[31] Stiebing K E, de Boer F W N, Fröhlich O, Bokemeyer H, Müller K A, Bethge K, and van Klinken J 2004 *J. Phys. G: Nucl. Part. Phys.* **30** 165